0022-3565/09/3293-908–918
THE JOURNAL OF PHARMACOLOGY AND EXPERIMENTAL THERAPEUTICS
U.S. Government work not protected by U.S. copyright
JPET 329:908–918, 2009

Vol. 329, No. 3
152017/3473809
Printed in U.S.A.

Selective Inhibitors of CYP2J2 Related to Terfenadine Exhibit Strong Activity against Human Cancers in Vitro and in Vivo[S]

Chen Chen, Guiling Li, Wanmin Liao, Jun Wu, Liu Liu, Ding Ma, Jianfeng Zhou, Reem H. Elbekai, Matthew L. Edin, Darryl C. Zeldin, and Dao Wen Wang

Department Internal Medicine and the Institute of Hypertension, Tongji Hospital, Tongji Medical College, Huazhong University of Science and Technology, Wuhan, People's Republic of China (C.C., G.L., W.L., J.W., L.L., D.M., J.Z., D.W.W.); and Division of Intramural Research, National Institute of Environmental Health Sciences, National Institutes of Health, Research Triangle Park, North Carolina (R.H.E., M.L.E., D.C.Z.)

Received February 10, 2009; accepted March 12, 2009

ABSTRACT

The cytochrome P450 epoxygenase, CYP2J2, converts arachidonic acid to four regioisomeric epoxyeicosatrienoic acids (EETs). We found recently that this enzyme is dramatically up-regulated in a variety of established human carcinoma cell lines and in human cancerous tissue and promotes the neoplastic phenotype. In the present study, we tested the hypothesis that specific inhibitors of CYP2J2 related to the drug terfenadine are effective antitumor agents. Four of these inhibitors (compounds 4, 5, 11, and 26) were tested for effectiveness in vitro and in vivo. In Tca-8113 cells, the CYP2J2 inhibitors decreased EET production by approximately 60%, whereas they had no effect on CYP2J2 mRNA or protein expression. Compound 26 inhibited the proliferation of human tumor cells, reduced their ability to adhere, invade, and migrate, and attenuated activation of epithelial growth factor receptor signal and kinases and phosphatidylinositol 3 kinase/Akt pathways. Inhibition of CYP2J2 also significantly potentiated human tumor cell apoptosis and caused a corresponding increase in caspase-3 activity and change in expression of apoptosis-related proteins Bax and Bcl-2. In murine xenograft models using MDA-MB-435 cells, treatment with compound 26 significantly repressed tumor growth, decreased lung metastasis, and was associated with increased expression of the anticancer genes CD82 and nm23, without causing toxicity. These data suggest that CYP2J2 inhibitors hold significant promise for use in treatment of neoplastic diseases.

Cytochrome P450 (P450) epoxygenases actively metabolize arachidonic acid to four regioisomers of *cis*-epoxyeicosatrienoic acid (5,6-, 8,9-, 11,12-, and 14,15-epoxyeicosatrienoic acids) (EETs). Differences in the catalytic efficiencies of individual P450 isoforms result in different regio- and stereoselective EET product profiles (Capdevila et al., 2000; Zeldin, 2001; Kroetz and Zeldin, 2002). Most of the arachidonic acid epoxygenases are members of the CYP2 family and include members of the CYP2B, CYP2C, and CYP2J subfamilies. Although expressed primarily in the liver, many P450 enzymes are expressed in extrahepatic organs, including lung, kidney, and gastrointestinal tissues (Wu et al., 1996; Enayetallah et al., 2004). CYP2J2 is a major enzyme found in extrahepatic tissue, with predominant expression in the cardiovascular system, including endothelial cells (Node et al., 1999) and cardiomyocytes (Wu et al., 1996).

Each P450 epoxygenase isozyme produces all four EET regioisomers, but one or two usually are the predominant products (Karara et al., 1993; Wu et al., 1997). 11,12- and 14,15-Regioisomers are the predominant EETs produced by many different cells and tissues and account for 67 to 80% of total EETs produced by five purified and reconstituted rat

This work was supported in part by the China Natural Science Foundation Committee [Grants 30540087, 30430320]; the International Collaboration Project [Grant 2005DFA30880]; the 973 Program [Grants 2007CB512004, 2002CB513107]; and by the Intramural Research program of the National Institutes of Health National Institute of Environmental Health Sciences [Grant Z01 ES025034].

C.C., G.L., and W.L. contributed equally to this work.

Article, publication date, and citation information can be found at http://jpet.aspetjournals.org.
doi:10.1124/jpet.109.152017.

[S] The online version of this article (available at http://jpet.aspetjournals.org) contains supplemental material.

ABBREVIATIONS: P450, cytochrome P450; EET, epoxyeicosatrienoic acid; DMEM, Dulbecco's modified Eagle's medium; FBS, fetal bovine serum; RT, reverse transcriptase; PCR, polymerase chain reaction; MTT, 3-(4,5-dimethylthiazol-2-yl)-2,5-diphenyltetrazolium; EGFR, epithelial growth factor receptor; PI3, phosphatidylinositol 3; HEK, human embryonic kidney; BAEC, bovine aortic endothelial cell; C26, compound 26; compound 11, 1-(4-bromophenyl)-4-[4-(hydroxydiphenylmethyl)-1-piperidinyl]-1-butanone; GAPDH, glyceraldehyde-3-phosphate dehydrogenase; 14,15-DHET, 14,15-dihydroxyeicosatrienoic acid; PBS, phosphate-buffered saline; ELISA, enzyme-linked immunosorbent assay; 20-HETE, 20-hydroxyeicosatetraenoic acid; HPF, high-power field; FITC, fluorescein isothiocyanate; TUNEL, terminal deoxynucleotidyl transferase dUTP nick-end labeling.

epoxygenases (Capdevila et al., 2000). Until now, little evidence shows that there are different biological properties among different EETs.

A myriad of studies have documented the role of EETs in the maintenance of cardiovascular health. In the heart, EETs activate K^+ channels, serve as endogenous regulators of cardiac electrical excitability, shorten the cardiac action potential, and confer cardioprotection after ischemia/reperfusion (Seubert et al., 2004). EETs are potent vasodilators and mediate the vasodilator responses to acetylcholine and bradykinin (Roman, 2002). In addition to their vasodilatory effects, EETs possess potent anti-inflammatory effects and decrease the expression of vascular cell adhesion molecule-1 and E-selectin in cultured endothelial cells (Node et al., 1999). EETs are also potent inducers of angiogenesis (Wang et al., 2005).

Although angiogenesis is pivotal in the processes of wound healing and tissue regeneration, it is also implicated in the pathological growth of neoplastic tumors. In recent publications, we have highlighted a pivotal role for EETs in promoting the cancer phenotype of carcinoma cells. We have shown that addition of exogenous EETs or recombinant adeno-associated viral vector-mediated delivery of P450 epoxygenases markedly enhanced the proliferation of cancer cells in vitro and in vivo (Jiang et al., 2005). EETs also inhibited carcinoma cell apoptosis through up-regulation of the antiapoptotic proteins Bcl-2 and Bcl-XL and down-regulation of the proapoptotic protein Bax (Jiang et al., 2005). In addition to inducing tumor cell proliferation, both endogenously formed and exogenously applied EETs increased cancer cell motility, adhesion, invasion, prometastatic gene expression, and xenograft metastasis to the lungs. In contrast, antisense to CYP2J2 or nonspecific P450 inhibitors significantly attenuated these neoplastic phenotypes (Jiang et al., 2005, 2007). All the findings suggested that inhibition of CYP2J2-mediated EET biosynthesis may represent a novel approach for the treatment of human cancers (Jiang et al., 2005).

H_1 histamine receptor antagonists are classified as specific antagonists, such as terfenadine and astemizole, and nonspecific antagonists, such as diphenhydramine and triprolidine (Simons, 2004). The antiinflammatory activities of H_1-antihistamines occur through a variety of mechanisms (Ciprandi et al., 1999; Triggiani et al., 2001). Antiinflammatory effects such as the inhibition of the expression of cell adhesion molecules and the chemotaxis of eosinophils and other cells may involve down-regulation of the H_1-receptor-activated nuclear factor-κB, a ubiquitous transcription factor that binds to the promoter and enhancer regions of many genes that regulate the production of proinflammatory cytokines and adhesion proteins (Bakker et al., 2001). Terfenadines, which are associated with cardiac toxic effects, are no longer approved for use (Leurs et al., 2002). However, terfenadine may induce DNA damage and apoptosis in human melanoma cell lines through Ca^{2+} homeostasis modulation and tyrosine kinase activity, independently of H_1 histamine receptors (Jangi et al., 2006, 2008).

Derivatives of the drug terfenadine were shown recently to be selective, high-affinity inhibitors of human CYP2J2 (Lafite et al., 2006, 2007). However, the role of these inhibitors in ameliorating EET-mediated promotion of the neoplastic phenotype has yet to be examined. In the present study, we utilized some of these inhibitors and synthesized a novel terfenadine derivative as a hydrochloride salt. We subsequently investigated the potential effects of these compounds on a host of processes related to cancer cell behavior and tumor pathogenesis. These findings suggest that selective inhibitors of CYP2J2 markedly attenuate the neoplastic phenotypes of carcinoma cells and may represent a novel class of therapeutic agents for the treatment of human cancers.

Materials and Methods

Chemicals. TRIzol and cell culture medium and reagents, including Dulbecco's modified Eagle's medium (DMEM), RPMI 1640 medium, trypsin, and fetal bovine serum (FBS), were purchased from Life Technologies (Carlsbad, CA). Reverse transcriptase (RT)-polymerase chain reaction (PCR) kit was from Takara (Kyoto, Japan). 11,12-EET, 3-(4,5-dimethylthiazol-2-yl)-2,5-diphenyltetrazolium (MTT), and collagen IV were purchased from Sigma-Aldrich (St. Louis, MO). Matrigel was purchased from BD Biosciences (San Jose, CA). Antibodies against epithelial growth factor receptor (EGFR), p-EGFR, phosphatidylinositol 3 (PI3) kinase, Bcl-2, Bax, CD82, nm23, and β-actin were purchased from Santa Cruz Biotechnology, Inc. (Santa Cruz, CA). Antibodies against AKT and p-AKT were purchased from Cell Signaling Technology Inc. (Danvers, MA). Horseradish peroxidase-conjugated secondary antibodies (goat anti-mouse IgG and goat anti-rabbit IgG) were purchased from KPL, Inc. (Gaithersburg, MA). Enhanced chemiluminescence reagents were purchased from Pierce Chemical (Rockford, IL); polyvinylidene difluoride membranes, prestained protein markers, and SDS-polyacrylamide gel electrophoresis gels were from Bio-Rad (Hercules, CA). All other reagents were purchased from standard commercial suppliers unless otherwise indicated.

Cell Lines. The Tca-8113 human tongue squamous cell carcinoma line, A549 human alveolar basal epithelial carcinomic cell line, HepG2 human hepatoma liver cell line, HeLa human cervix carcinoma cell line, HEK293 human kidney epithelial cell line, and H9c2 rat myocardium cell line were obtained from the American Type Culture Collection (Manassas, VA) and maintained as recommended by the source. Cells were cultured in DMEM, adjusted to contain 4 mM L-glutamine, 1.5 g/l sodium bicarbonate, 4.5 g/l glucose, 10% FBS, 100 units/ml penicillin, and 65 units/ml streptomycin. The TC-1 mouse lung epithelial carcinomic cell line and MDA-MB-435 human breast carcinoma cell line were also obtained from the American Type Culture Collection and were maintained in RPMI 1640 medium, supplemented with 4 mM L-glutamine, 1.5 g/l sodium bicarbonate, 4.5 g/l glucose, 10% FBS, 100 units/ml penicillin, and 65 units/ml streptomycin. All cell lines were maintained at 37°C in a humidified incubator containing 5% CO_2.

Isolation and Culture of Bovine Aortic Endothelial Cells. Fresh bovine thoracic aortas were obtained from a local slaughterhouse, and bovine aortic endothelial cells (BAECs) were harvested using trypsin (0.25%) and cultured as described previously (Wang et al., 2005). In brief, BAECs were grown to confluence in DMEM supplemented with 4 mM L-glutamine, 1.5 g/l sodium bicarbonate, 1.0 g/l glucose, 15% FBS, and an antibiotic mixture of 100 units/ml penicillin and 100 μg/ml streptomycin. Purity of the BAEC preparation was determined by cell morphology using phase-contrast microscopy and by immunofluorescent staining for CD31 (~90%). Cells were maintained at 37°C in a humidified incubator containing 5% CO_2. All passages were performed using 0.05% trypsin and 0.02% EDTA. Only cells passaged less than five times were used for experiments.

Synthesis of Terfenadone Derivatives. The design and synthesis of high-affinity and selective CYP2J2 inhibitors derived from terfenadone, a derivative of the drug terfenadine, have been described in detail by Lafite et al. (2007). We synthesized three of these compounds (compounds 4, 5, and 11), and an additional novel compound, which we have labeled compound 26 (C26), as hydrochloride

salts. A schematic description for the synthesis of these compounds is shown in Scheme 1. In brief, substituted benzene derivatives and 4-chlorobutanoyl chloride were added progressively to a cold solution of CH_2Cl_2 and $AlCl_3$. After stirring at 0°C for 2 h, the mixture was poured into ice water and stirred. After complete melting of the ice water, CH_2Cl_2 was again added to the solution. The organic phase was then separated, and the aqueous phase was extracted with CH_2Cl_2. The extract was dried ($NaSO_4$), and the solvent was evaporated under vacuum. The resulting 4-chloro-1-butanone derivatives were added to a dry flask with α,α-diphenyl-4-piperidinomethanol, $KHCO_3$, KI, and toluene. The mixture was refluxed for 72 h, after which the solvent was evaporated under heating, and the residue was washed with water. The organic layers were then concentrated under vacuum.

Synthesis of C26. Chloromethylbis(triphenylphosphine) palladium and vinyltributyltin were added to a mixture of compound 11 in a solution of hexamethylphosphoramide. The yellow solution was heated to 65°C with constant stirring in a sealed tube until the solution turned black (1–2 h). After cooling to room temperature, 5 ml of H_2O was added. The resulting mixture was extracted with ether and washed with water. The combined extract was dried with Na_2SO_4. After evaporation of the solvent, the crude product was purified by distillation. The resulting oil was dissolved in ether, and hydrochloric acid was added to precipitate the product. The precipitate was filtered and washed with ethyl acetate.

Analysis of CYP2J2 Expression by RT-PCR. Total RNAs were isolated from cell cultures 24 h after treatment with 10 μM CYP2J2 inhibitors using TRIzol reagent. Semiquantitative analysis of the expression of CYP2J2 mRNA was done using a multiplex RT-PCR technique. Expression of glyceraldehyde-3-phosphate dehydrogenase (GAPDH) mRNA was used as an internal standard. RNA was reverse-transcribed using the Takara Bio RT-PCR kit (Takara Bio USA, Madison, WI), according to the manufacturer's protocol. The PCR reaction mixture contained 5 μl of cDNA, 1× PCR buffer, 1.5 mM $MgCl_2$, 0.8 mM deoxynucleotide triphosphates, 1 unit of Taq DNA polymerase, and 100 nM each primer for CYP2J2 (sense

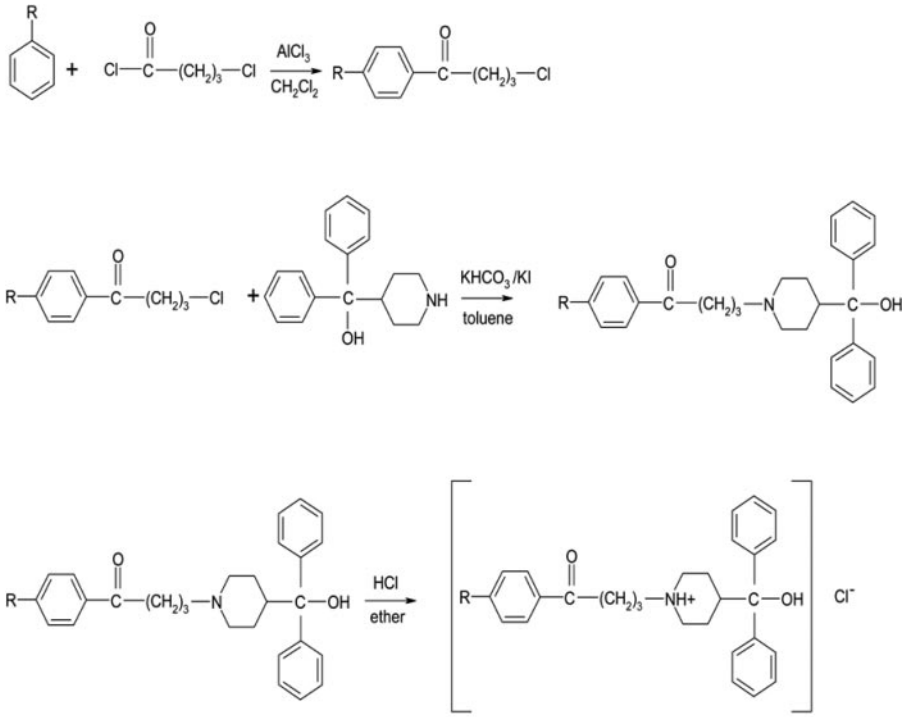

Scheme 1. Synthesis of terfenadone derivatives. The schematic shows synthesis and chemical structures of compounds 4, 5, 11, and 26.

Inhibitor	–R
Terfenadine	
C4	$-CH_2-CH_2-CH_3$
C5	$-CH_2-CH=CH_2$
C11	–Br
C26	$-CH=CH_2$

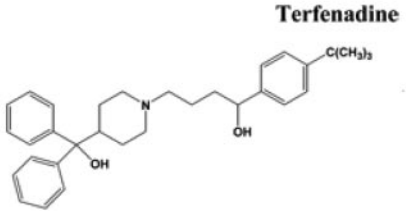

primer, 5′-CTCCTACTGGGCACTGTCGC-3′; antisense primer, 5′-TGGGCCTCCTCCTGAAT-3′) or for GAPDH (sense primer, 5′-ACCACAGTCCATGCCATCAC- 3′; antisense primer, 5′-TCCACCACCCTGTTGCTGTA-3′). After 35 cycles, PCR products were resolved in 1% agarose gels stained with ethidium bromide. The relative intensity of CYP2J2 compared with GAPDH was calculated for each sample by densitometry.

Analysis of Protein Expression and Phosphorylation by Western Blotting. Proteins from cell lysates (20 μg) were separated by 8% SDS-polyacrylamide gel electrophoresis and transferred to a polyvinylidene difluoride membrane. After blocking in 5% nonfat milk, protein blots were incubated with a specific antibody followed by incubation with a peroxidase-conjugated secondary antibody in blocking buffer. The bands were visualized with the enhanced chemiluminescence method according to manufacturer's instructions (Pierce Chemical). Polyclonal antibodies against CYP2J2 were developed as described previously (Wu et al., 1996) and showed no cross-reactivity with other P450 isoforms.

Determination of 14,15-Dihydroxyeicosatrienoic Acid Levels. For the measurement of the stable EET metabolite 14,15-dihydroxyeicosatrienoic acid (14,15-DHET) in cultured cells, cells were scraped in ice-cold PBS, pH 7.2, with triphenylphosphine after washing with PBS and then homogenized and sonicated over ice, as described previously (Jiang et al., 2005; Yang et al., 2007). For the measurement of 14,15-DHET in urine of nude mice, the urine was preserved with triphenylphosphine and stored at −80°C until use. Eicosanoids were extracted from the cell homogenates and urine thrice with ethyl acetate after acidification with acetic acid. After evaporation, the samples were dissolved in *N*,*N*-dimethylformamide (AMRESCO Inc., Solon, OH), and the concentration of 14,15-DHET was determined by an ELISA kit (R&D Systems, Minneapolis, MN), according to the manufacturer's instructions.

Determination of 20-Hydroxyeicosatetraenoic Acid Levels. For measurement of 20-hydroxyeicosatetraenoic acid (20-HETE) in cultured cells, cells were scraped in cold PBS, pH 7.2, with triphenylphosphine after washing with PBS and then homogenized and sonicated over ice. 20-HETE was also measured in the urine of nude mice, which was preserved with triphenylphosphine and stored at −80°C until use. The concentration of 20-HETE was determined by an ELISA kit (R&D Systems) according to the manufacturer's instructions.

Growth Inhibition Assays. Growth inhibition studies in Tca-8113, HeLa, A549, HepG2, MDA-MB-435, TC-1, and HEK293 cell lines, primary BAECs, and neonatal rat primary cardiomyocytes were performed using the MTT assay as described previously (Jiang et al., 2005). This assay measures the conversion of MTT to formazan crystals by enzymes in the mitochondria of metabolically active cells. For these studies, cells seeded at 1×10^4 cells/well (quintuplicate repeats in 96-well plates) were allowed to attach for 24 h. At 60% confluence, the medium was removed, and the cells were washed thrice with PBS and incubated with serum-free medium at 37°C for 24 h to allow for synchronization. Cells were treated with CYP2J2 inhibitors (10 μM) for various time periods from 4 to 24 h every 4 h. After treatment with MTT, the formed crystals were dissolved in dimethyl sulfoxide, and the intensity of the color in each well was measured at a wavelength of 490 nm using a microplate reader. Before these experiments, we tested doses of CYP2J2 inhibitor C26 ranging from 10 nM to 100 μM in these cell lines to define the proper dose by antiproliferation effect. Results showed that C26 dose-dependently inhibited human carcinoma cell growth from 0.5 to 20 μM, and 5 and 10 μM C26 showed the best cell growth inhibition effect (Supplemental Fig. 1) without effect on CYP2J2-negative cells, including HEK293 cells and TC-1 (mouse lung cancer cells). Therefore, these doses were chosen for further experiments.

Ki67 Immunohistochemistry. Cells were loaded onto slides, plated in six-well plates at 1×10^6 cells/well, and allowed to attach for 24 h. After growth to 60% confluence, the medium was removed, and the cells were washed thrice with PBS and incubated with serum-free medium at 37°C for 24 h to allow for synchronization. Cells were then treated with CYP2J2 inhibitors (10 μM) for 24 h and then fixed with formaldehyde. After Cytonin antigen retrieval, slides were incubated with the Ki67 antibody for 16 h at 4°C. Slides were washed thrice (15 min each) with PBS at room temperature and then incubated with a secondary antibody for 1 h at room temperature. After three more

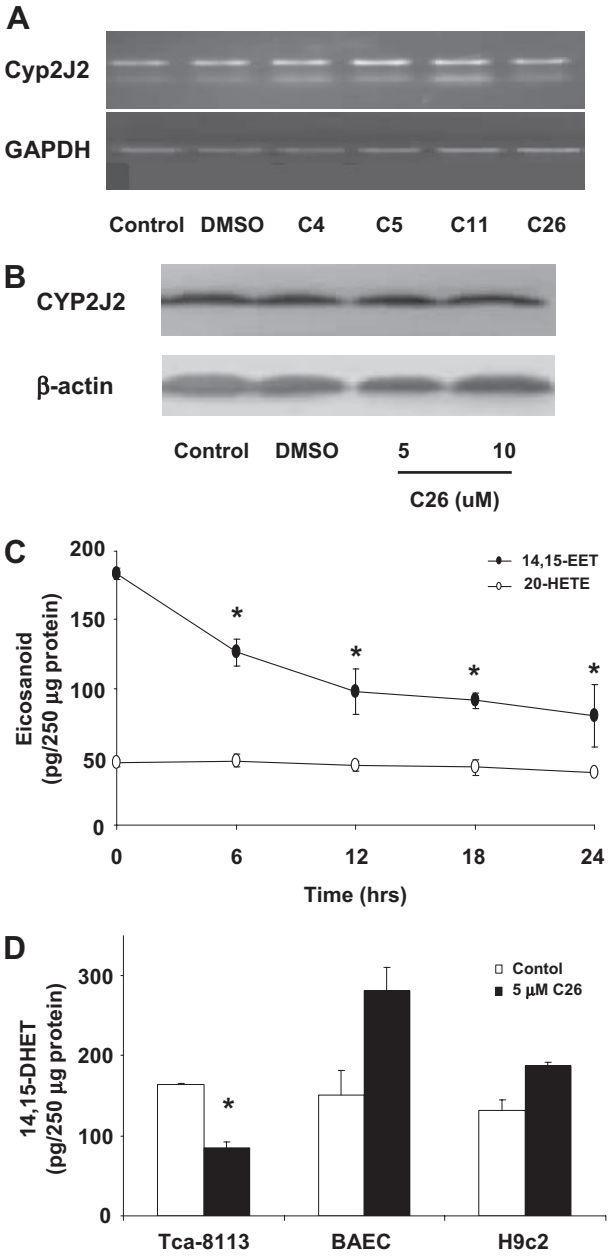

Fig. 1. Effect of terfenadone derivatives on CYP2J2 expression and activity. A, CYP2J2 mRNA levels. Total RNAs were isolated from Tca-8113 cells treated with compounds 4, 5, 11, and 26 (10 μM each) for 24 h. Semiquantitative analysis of the expression of CYP2J2 mRNA was done using a multiplex RT-PCR technique as described under *Materials and Methods*. B, CYP2J2 protein levels. Tca-8113 cells were treated with 5 or 10 μM C26 for 24 h. Proteins from cell lysates were then subject to Western blot analysis as described under *Materials and Methods*. C, 14,15-DHET and 20-HETE levels in Tca-8113 cells. Levels of 14,15-DHET and 20-HETE were determined as described under *Materials and Methods* over a 24-h period after treatment of cells with C26 (10 μM). D, 14,15-DHET levels in BAECs, H9C2 and Tca-8113 cells. 14,15-DHET levels in cells treated with C26 (5 μM) for 24 h were determined. Results shown are mean ± S.E. ($n = 5$); *, $p < 0.05$ versus control, representative of three independent experiments.

washes with PBS (15 min each) at room temperature, immunostaining was visualized with diaminobenzidine (Sigma-Aldrich). Slides were scanned under an inverted microscope (Nikon TE 2000; Nikon, Tokyo, Japan) equipped with digital imaging. For each treatment, 10 high-power field (HPF) images were captured.

Colorimetric Assay for the Measurement of Caspase-3 Activity. Caspase-3 activity was measured using a colorimetric assay kit according to manufacturer's instructions (R&D Systems). In brief, treated cells were collected and lysed by the addition of lysis buffer. After centrifugation, a caspase-specific peptide that was conjugated to a color reporter molecule and reaction buffer were added to the supernatant and incubated at 37°C for 2 h in the dark. Release of the chromophore by the caspase enzymatic activity was quantified spectrophotometrically at a wavelength of 405 nm.

Determination of Apoptosis by Flow Cytometry. Cells were seeded into six-well plates at 1×10^6 cells/well and allowed to attach for 24 h. At 60% confluence, the medium was removed, and the cells were washed thrice with PBS and incubated with serum-free medium at 37°C for 24 h to allow for synchronization. After treatment with the C26 (10 μM) for 6, 12, 18, and 24 h, cells were harvested with trypsin/EDTA, resuspended in binding buffer, and incubated with FITC-conjugated annexin V and propidium iodide according to the manufacturer's protocol (Annexin V-FITC kit; Bender MedSystems Inc., Burlingame, CA). Cells were then analyzed with a FACStar-Plus flow cytometer (BD Biosciences, Franklin Lakes, NJ).

TUNEL Assay. Cells were loaded onto slides, plated in six-well plates at 1×10^6 cells/well, and allowed to attach for 24 h. After growth to 60% confluence, the medium was removed, and the cells were washed thrice with PBS and incubated with serum-free medium at 37°C for 24 h to allow for synchronization. Cells were then treated with compounds 4, 5, 11, and 26 for 24 h (10 μM) and then fixed with fresh 4% paraformaldehyde at room temperature for 10

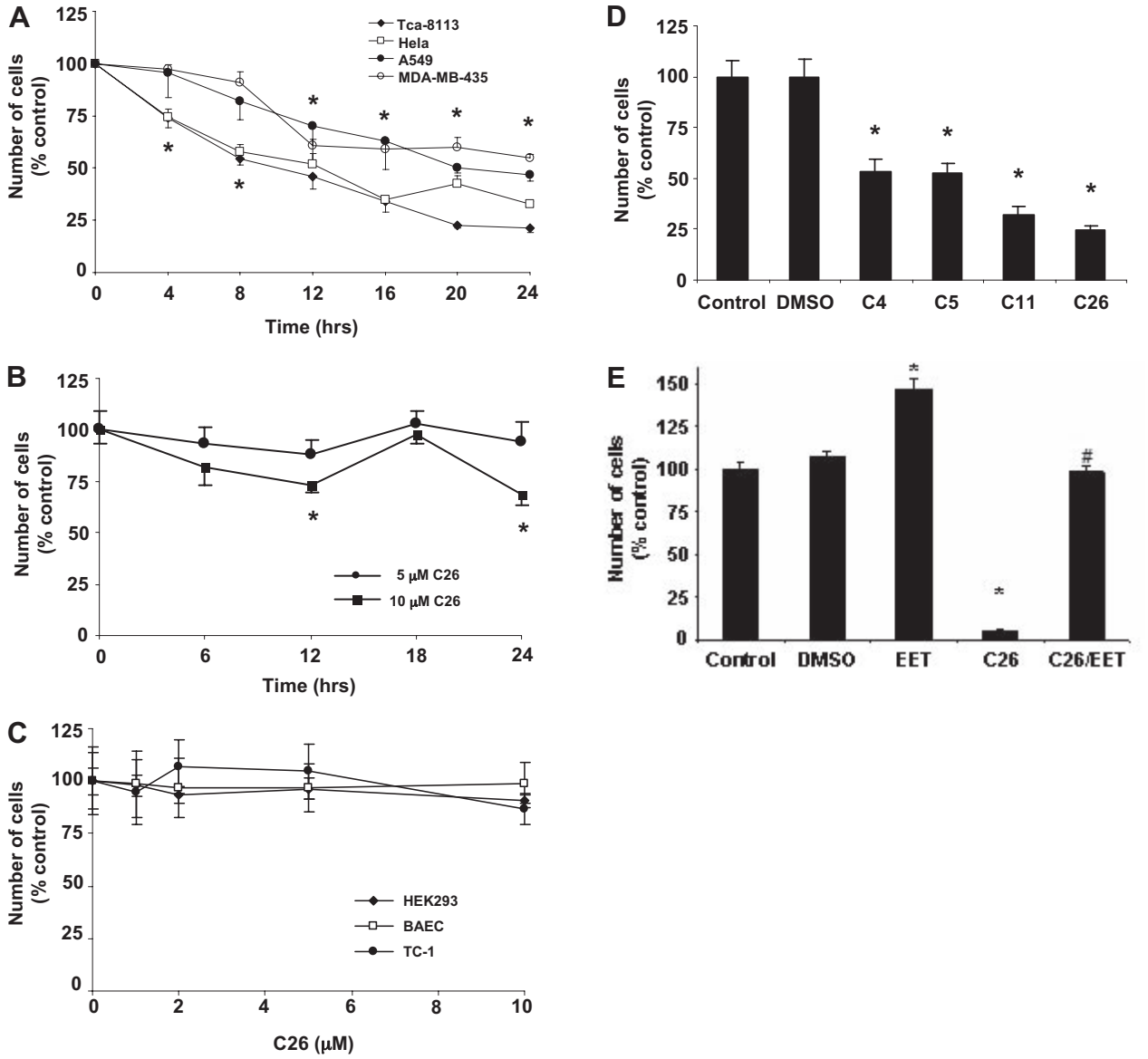

Fig. 2. Effect of CYP2J2 inhibitors on cell proliferation. A, effect of C26 (10 μM) on number of Tca-8113, HeLa, A549 and MDA-MB-435 tumor cells. B, effect of C26 on number of HepG2 cells. C, effect of C26 (10 μM) on number of HEK293 cells, BAECs, and TC-1 cells. D, effect of CYP2J2 inhibitors on number of Ki67 immunopositive Tca-8113 cells. Cells were treated with vehicle and one of the CYP2J2 inhibitors (10 μM each), and the numbers of Ki67-positive cells per HPF were determined as described under *Materials and Methods*. E, effect of 11,12-EET (200 nM) on the antiproliferative effect of C26 (10 μM) in Tca-8113 cells. Growth inhibition studies for A, B, C, and E were performed using the MTT assay, as described under *Materials and Methods*. Data are expressed as percentage of untreated controls, which is set at 100% ± S.E. ($n = 5$); *, $p < 0.05$ versus control; #, $p < 0.05$ versus C26.

min. The In Situ Apoptosis Detection Kit was used according to the manufacturer's instructions (R&D Systems). The slides were scanned under an inverted microscope (Nikon TE 2000) equipped with digital imaging. For each treatment, 10 HPF images were captured.

Fibronectin Adhesion Assay. Adhesion of cells to fibronectin was carried out as described previously (Zipin et al., 2004). In brief, nontissue culture 96-well plates were coated with 100 μl/well of 10 μg/ml fibronectin for 60 min at 37°C and blocked twice with 200 μl of 1% bovine serum albumin in phenolsulfonphthalein-free medium for 30 min at 37°C. Cells (1×10^4), in 100 μl of phenolsulfonphthalein-free medium containing 0.1% bovine serum albumin, treated with or without C26 (10 μM), were added to fibronectin-coated wells for 60 min at 37°C. After three washes with medium to remove nonadhered cells, the cells were covered with 100 μl of phenolsulfonphthalein-free medium, and 10 μl of MTT solution (5 mg/ml) was added for cell count determination (Jiang et al., 2005). Absorbance values at 490 nm reflect the proportional number of cells adhering to fibronectin.

Cell Migration and Invasion Assays. Chemotactic migration was evaluated using a modified Boyden chamber as described previously (Fishman et al., 2001). Porous filters (8-μm pores) were coated by passive adsorption for 24 h with type IV collagen (10 μg/ml collagen in coating buffer; Sigma-Aldrich). Cells (1×10^6) were then plated in the upper chamber, whereas 5% FBS-supplemented medium was added to the bottom chamber to act as a chemoattractant. Subsequently, serum-free medium with compounds 4, 5, 11, or 26 (10 μM) was added to the upper chamber, and cells were allowed to migrate for up to 4 h. Nonmigrating cells were removed from the upper chamber, with a cotton swab and filters were stained with DiffQuik stain. Migrating cells adherent to the underside of the filter were counted with an ocular micrometer, counting a minimum of 10 HPFs. To study cell invasiveness, cells (1×10^6) were plated onto Boyden chambers coated with Matrigel (500 μg/filter) and incubated for 4 h. Chambers were stained as described above and invasiveness was evaluated by quantifying the number of cells invading the Matrigel assay and reaching the opposite side of the filter. All the data are expressed as relative migration (number of cells per field) and represent the mean ± S.E. of quadruplicate experiments.

In Vivo Antitumor Activity. Athymic BALB/c mice, 4 weeks of age, were housed in a 12-h light/dark cycle in a pathogen-free environment and allowed ad libitum access to food and water. All animal studies were approved by the Animal Research Committee of Tongji Medical College and done according to the NIH *Guide for the Care and Use of Laboratory Animals* (National Research Council, 1996). MDA-MB-435 cells, cultured in log-phase growth, were harvested on the day of use and inoculated into the right flank of male athymic BALB/c mice. After inoculation of tumor cells, mice were monitored daily and weighed weekly. Digital caliper measurements were begun when tumors became visible. When tumors had grown to approximately 40 mm^3, approximately 14 days after implantation, tumor-bearing mice were randomized into control and drug treatment groups ($n = 6$). C26 dissolved in dimethyl sulfoxide was administered orally for 30 days at a dose of 0.25 mg/kg/day. At the end of the experiment, mice were sacrificed by sodium pentobarbital overdose (90 mg/kg i.p.), and primary tumors were removed and weighed. Tumor volumes were calculated as length × width^2 × π/6 as described previously (Bajo et al., 2002). Lungs were also removed for quantification of white metastatic colonies on the lung surfaces.

The effect of C26 on lung metastasis and survival was also assessed. Cells were harvested and inoculated into the right flank of male athymic BALB/c mice as described above. C26 or vehicle was administrated orally for up to 11 weeks at a dose of 0.25 mg/kg/day. Lungs were removed for quantification of white metastatic colonies on the lung surfaces and primary tumors were removed, weighed, and analyzed by immunoblotting.

Before these experiments, we tested doses of C26 from 0.05 to 1 mg/kg/day in tumor-bearing athymic BALB/c mice to define the proper dose by antitumor growth. Results showed that 0.25 mg/kg/day C26 had the significant effect (data not shown), and this dose was chosen for the further in vivo experiment.

Statistics. Data are presented as mean ± S.E. The Wilcoxon test, Student's *t* test, or analysis of variance was performed to determine statistical significance of differences among treatment groups, as appropriate. In all cases, statistical significance was defined as $p < 0.05$.

Results

Design and Synthesis of Selective CYP2J2 Inhibitors. We synthesized a series of small-molecule, high-affinity, selective inhibitors of CYP2J2 based on previously published methods (Lafite et al., 2006, 2007). The compounds were related to terfenadone, a derivative of the drug terfenadine, and synthesized as hydrochloride salts for ease of administration (Scheme 1). Specifically, we chose compounds 4 (-CH_2-CH_2-CH_3), 5 (-CH_2-CH = CH_2), and 11 (-Br) because of their low IC_{50} values for CYP2J2 (~0.4 μM), which were 14- to 20-fold higher than for other P450s (Lafite et al., 2007). In addition to these three compounds, we designed and synthesized a novel inhibitor, C26, for which we used a vinyl moiety (-CH = CH_2) as the substitute group. The chemical structures of all four compounds were established from their ^{1}H NMR and mass spectra; ^{1}H NMR spectroscopy analyses in the presence of an internal standard showed that all four compounds were greater than 95% pure.

Terfenadone Derivatives Inhibit the Activity of CYP2J2 but Do Not Affect Its Expression. To verify that the synthesized terfenadone derivatives inhibit the activity of CYP2J2, but not its expression, we examined mRNA and protein levels of CYP2J2 in Tca-8113 cells after treatment with the four compounds for 24 h (10 μM). As expected, none of the inhibitors altered mRNA or protein expression of CYP2J2 (Fig. 1, A and B). Similar results were obtained with all six tumor cell lines and three nontumor cells (data not shown). Lafite et al. (2006, 2007) previously have established the specificity of terfenadone derivatives for inhibition of CYP2J2. To confirm inhibition of P450 epoxygenase but not ω-hydroxylase activity by these compounds, we measured the levels of the stable EET metabolite 14,15-DHET and the ω-hydroxylase metabolite 20-HETE in cell homogenates. 14,15-DHET levels, but not 20-HETE levels, were significantly decreased in Tca-8113 cells after treatment with C26 in a time-dependent fashion (Fig. 1C). In cells with non-CYP2J2 expression (e.g., BAECs, H9c2 cells), 14,15-DHET levels were not significantly altered in the presence of C26 (10 μM) for 24 h, verifying the specificity of this inhibitor toward CYP2J2 activity (Fig. 1D).

CYP2J2 Inhibitors Decrease Human Tumor Cell Proliferation. As a first step in establishing the effect of CYP2J2 inhibitors, we determined the effect of C26 (10 μM) on proliferation of cells in vitro over a 24-h time period. C26 caused a significant, time-dependent decrease in the number of viable Tca-8113, HeLa, A549, and MDA-MB-435 cells, as determined by the MTT assay (Fig. 2A). On the other hand, in HepG2 cells, which express lower levels of CYP2J2 than other human tumor cells, inhibition of CYP2J2 by C26 caused a significant, albeit less profound, decrease in cell number (Fig. 2B). In contrast, in human nontumor cells (HEK293) and in nonhuman tumor and nontumor cells (TC-1, BAECs) that do not express

CYP2J2, increasing doses of C26 had no significant effect on cell number (Fig. 2C). Furthermore, all four inhibitors (10 μM) decreased the number of Ki67-positive Tca-8113 cells (Fig. 2D). It is not surprising that addition of exogenous 11,12-EET (200 nM) attenuated the antiproliferative effect of C26 (10 μM), confirming the role of EETs in promoting cell proliferation (Fig. 2E).

CYP2J2 Inhibitors Activate Caspase-3 and Enhance Human Tumor Cell Apoptosis. Given the observed effects on tumor cell proliferation, it was of interest to determine the effect of CYP2J2 inhibitors on the apoptosis of cancer cells. Using a colorimetric assay, we determined the effect of C26 (5 and 10 μM) on the activity of caspase-3, an intracellular cysteine protease that exists as a proenzyme and becomes activated during the cascade of events associated with apoptosis (Roy et al., 2001). C26 significantly increased caspase-3 activity in Tca-8113 cells in a dose-dependent manner (Fig. 3A). Apoptotic Tca-8113 cells were then identified by TUNEL staining after treatment with compounds 4, 5, 11, and 26 (10 μM) for 24 h. As shown in Fig. 3B, the four inhibitors significantly increased the number of TUNEL-positive cells, although the increase was more pronounced in cells treated with compounds 4, 5, and 26. In addition, C26 (10 μM) increased the number of annexin V-positive cells over a 24-h period (Fig. 3C).

CYP2J2 Inhibitors Reduce Human Tumor Cell Adhesion, Migration, and Invasion. The effect of CYP2J2 inhibitors on metastatic potential of cancer cells was assessed in vitro by examining adherence to fibronectin, migration, and invasion potential. The effect of C26 on the adhesion of Tca-8113 cells to fibronectin was assessed using the MTT assay. As shown in Fig. 4A, C26 (5 and 10 μM) significantly reduced the number of cells adhering to fibronectin after 2 h of treatment. Similar results were obtained when cells were treated with 10 μM of compounds 4, 5, or 11 (Fig. 4B).

The effect of CYP2J2 inhibitors on cell migration was assessed in two cancer cell lines. C26 inhibited cell migration in a dose- and time-dependent manner (Fig. 4, C and D). In addition, the presence of 11,12-EET (200 nM) attenuated the inhibitory effect of C26 (10 μM) on cell migration, confirming the role of EETs in promoting the metastatic phenotype of cancer cells and verifying that the antineoplastic properties of C26 stem from its inhibitory effect on CYP2J2 (Fig. 4E). In agreement with the results of migration assays, inhibition of CYP2J2 by the inhibitors significantly decreased the number of cells invading into Matrigel assay (Fig. 4F).

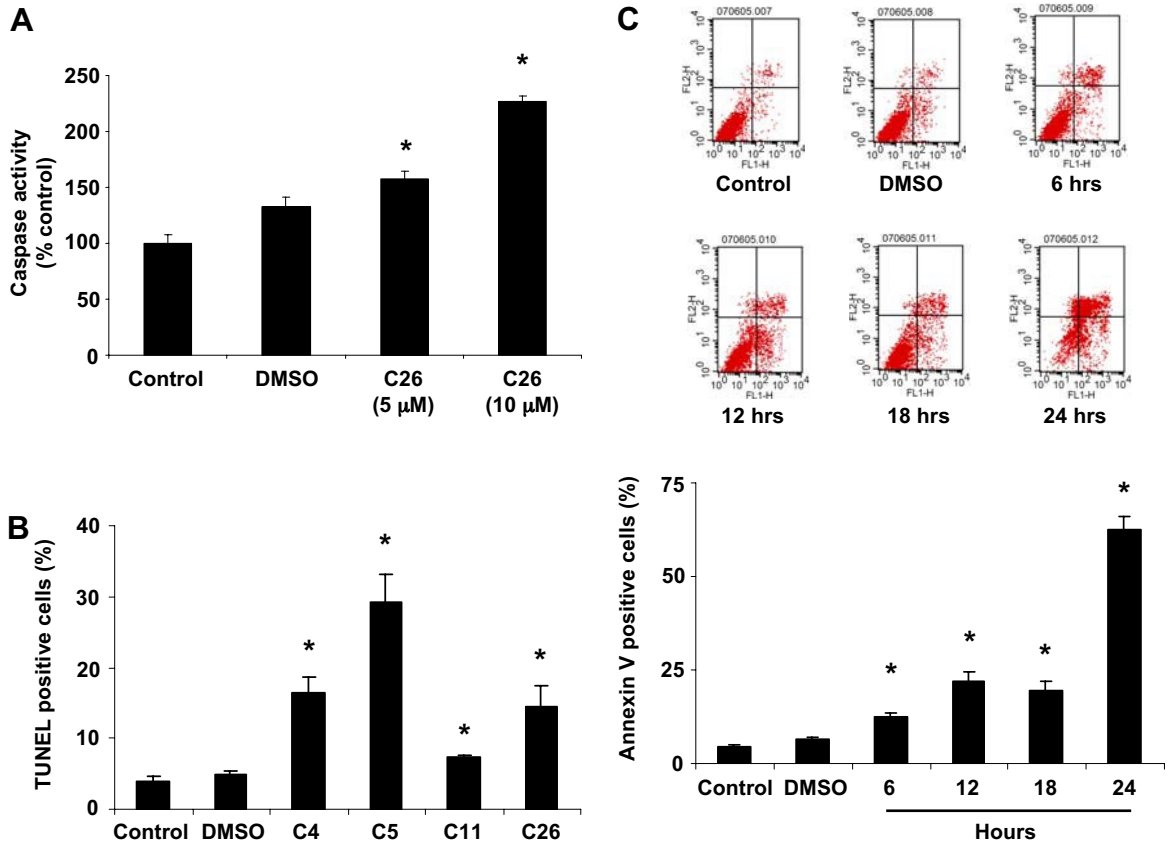

Fig. 3. C26 increases human tumor cell apoptosis. A, caspase-3 activity in Tca-8113 cells. Cells were treated with 5 and 10 μM C26 for 18 h, lysed, and analyzed spectrophotometrically for caspase activity. Data are reported as mean absorption relative to control ± S.E. ($n = 3$). B, identification of apoptotic cells by TUNEL staining. Tca-8113 cells were treated with compounds 4, 5, 11, and 26 for 24 h and then fixed with paraformaldehyde. DNA fragments and double-strand breaks in apoptotic cells were labeled with biotinylated nucleotides and detected using the In Situ Apoptosis Detection Kit. Apoptotic cells with their characteristic fragmented chromatin exhibit a dark-blue nuclear staining. Graph represents quantification of the percentage of cells that were TUNEL positive. Data are reported as mean ± S.E. ($n = 5$). C, analysis by flow cytometry of Tca-8113 cells treated with C26 (10 μM) using annexin V-FITC and propidium iodide. The lower left quadrant represents nonapoptotic cells, the lower right quadrant is representative of early apoptotic cells (annexin positive, propidium iodide negative), and the upper right quadrant represents annexin V and propidium iodide-positive late apoptotic or necrotic cells. Graph represents the mean number of annexin-positive Tca-8113 cells expressed as percentage of control untreated cells ± S.E. ($n = 3$); *, $p < 0.05$ versus control.

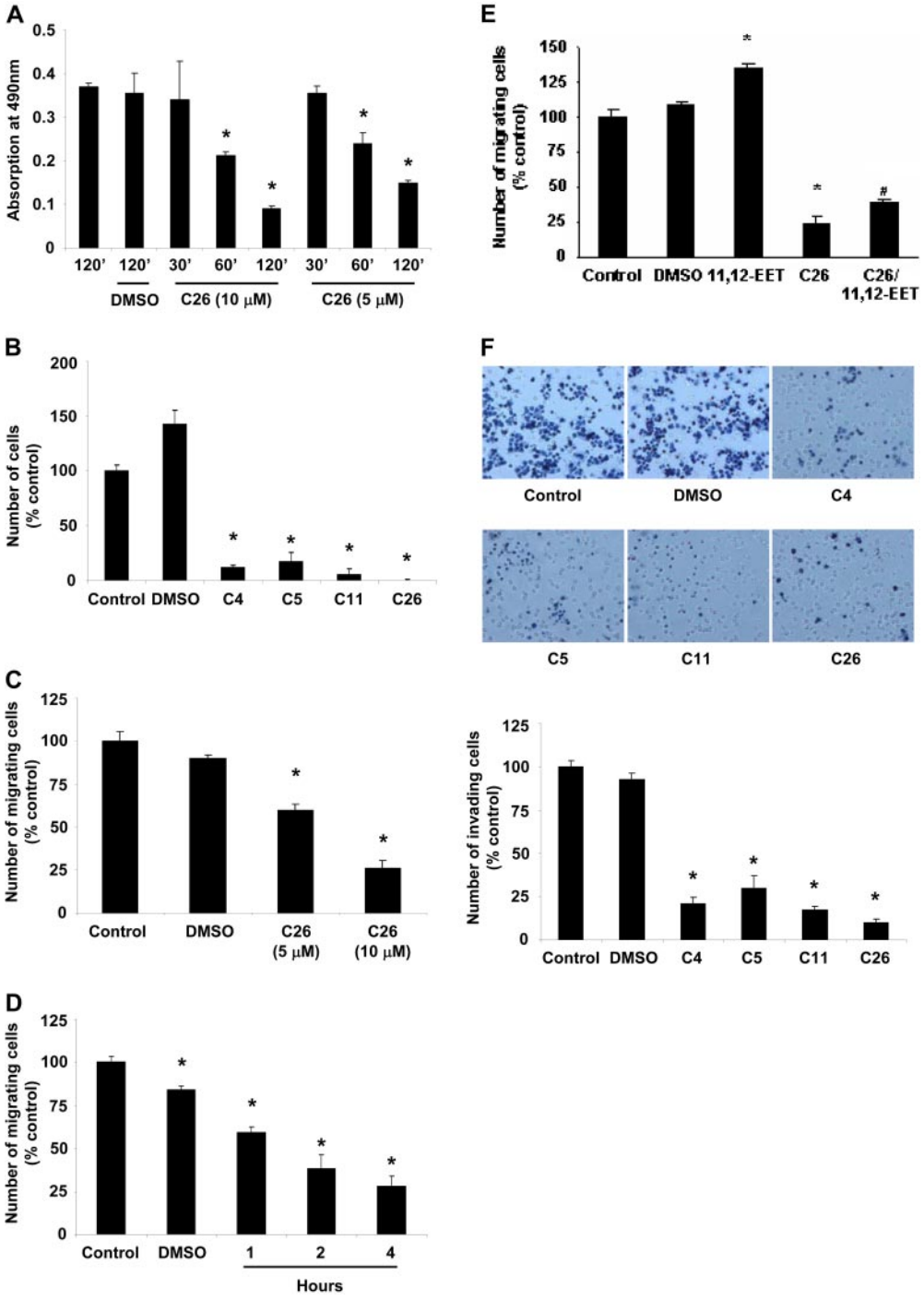

Fig. 4. CYP2J2 inhibitors decrease the adhesion, migration, and invasion of Tca-8113 to fibronectin. A, number of cells adhering to fibronectin after treatment with 5 and 10 μM C26 for 30 min to 2 h. B, number of cells adhering to fibronectin 2 h after treatment with 10 μM compounds 4, 5, 11, or 26. Fibronectin adhesion assay was performed as described under *Materials and Methods*. C, migration of Tca-8113 cells treated with 5 and 10 μM C26 for 4 h. D, migration of MDA-MB-435 cells treated with 10 μM C26 over a 4-h time period. E, effect of 11,12-EET (200 nM) on the antimigratory effect of C26 (10 μM) in Tca-8113 cells. The Boyden chamber migration assay was performed as described under *Materials and Methods*. F, cells were treated with 10 μM compounds 4, 5, 11, or 26 for 4 h. Thereafter, invasiveness was evaluated by quantifying the number of cells invading the Matrigel in a Boyden chamber as shown. Data are expressed as percentage of untreated controls, which is set at 100% ± S.E. ($n = 5$); *, $p < 0.05$ versus control; #, $p < 0.05$ versus C26.

CYP2J2 Inhibitors Depress Murine Xenograft Tumor Growth and Metastasis. After our in vitro assessment of effects of CYP2J2 inhibitors, we examined the effect of CYP2J2 inhibitors on tumor growth in an in vivo MDA-MB-435 cell murine xenograft model. Athymic BALB/c mice were injected subcutaneously with 2×10^6 MDA-MB-435 cells/mouse, and the tumor was allowed to grow for 14 days before randomization of the animals to control or CYP2J2 inhibitor treatment groups ($n = 6$ for each group). During the treatment period, 14,15-DHET and 20-HETE urine levels were measured. As expected, C26 decreased 14,15-DHET levels but had no significant effect on 20-HETE levels (Fig. 5, A and B). The decrease in EET levels in the treatment group was paralleled by a decrease in tumor growth over a 28-day period (Fig. 5C). The difference in tumor volume between the control and treatment groups was apparent within 7 days after randomization of the animals but only became significant after 21 days. At the end of the treatment period, C26 was associated with decreased tumor weight, without change in body weight (Fig. 5D).

To confirm the effect of C26 on lung metastases and survival, we performed additional experiments. In the survival study, the control group died significantly earlier than the treatment group ($n = 10$ for each group) (Fig. 5E). In the metastasis experiment, all animals were sacrificed at 8 weeks, and lungs were removed to count metastatic tumor

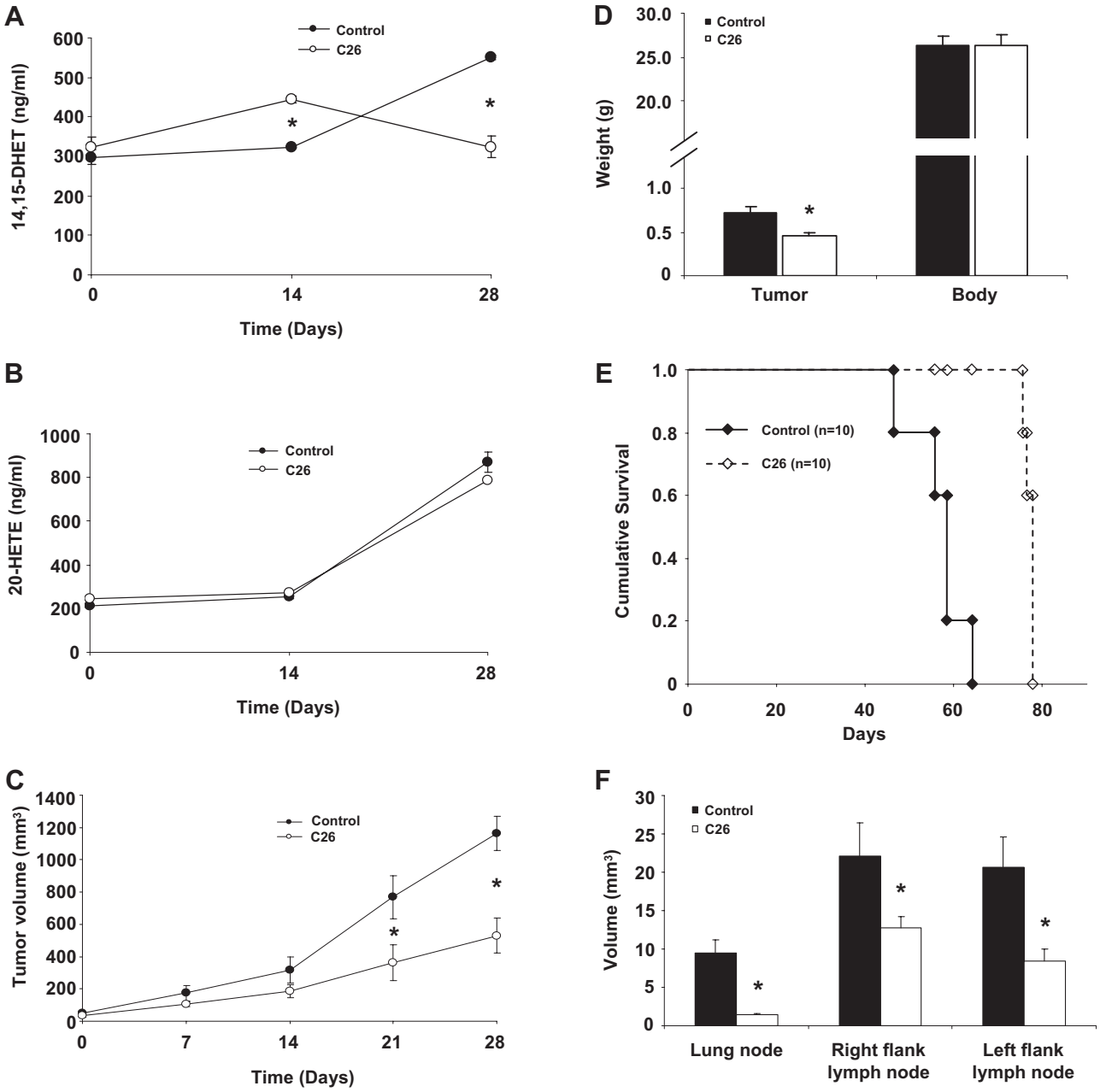

Fig. 5. Effect of C26 on tumor growth and metastasis. Athymic mice were inoculated with MDA-MB-435 cells, and the tumors were allowed to grow to approximately 40 mm^3. The mice were then randomized to control versus C26 treatment. Mice were dosed orally with vehicle or C26 (0.25 mg/kg/day) for 30 days. A, 14,15-DHET levels in the urine of nude mice during treatment with C26 or vehicle control ($n = 6$). B, 20-HETE levels in the urine of nude mice during treatment with C26 or vehicle control. 14,15-DHET and 20-HETE were detected by ELISA according to the manufacturer's instructions ($n = 6$). C, tumor volume as measured weekly in control and C26-treated mice. Tumor volume was monitored by digital caliper on a weekly basis and calculated as length $\times$ width^2 $\times$ $\pi/6$ ($n = 6$). D, tumor and body weight of mice 30 days after randomization into control and C26 treatment groups ($n = 6$). E, cumulative survival curve of control and C26-treated mice ($n = 10$). F, average volume of lung metastases for each group ($n = 6$). Results shown are mean $\pm$ S.E. ($n = 6$); $*$, $p < 0.05$ versus control.

colonies. It is interesting that we observed a significant decrease of number of metastases in mice treated with C26 compared with mice treated with vehicle ($n = 6$ for each group). Metastatic colonies were observed in the lungs from all 10 control mice but observed in only two of the C26-treated mice. Moreover, the average volume of lung metastases in C26-treated mice was significantly lower than in control mice (Fig. 5F). Together, these data indicate that C26 treatment can inhibit lung metastasis and prolong survival of tumor-bearing mice.

Histological, biochemical, and enzymatic assays did not reveal any significant toxicity in control or C26-treated animals. C26 treatment did not increase activity of liver enzymes (alanine aminotransferase and aspartate aminotransferase) or elevate serum urea nitrogen levels (Table 1). No obvious abnormalities were found in control or C26-treated liver, heart, aorta, or kidney tissues stained with hematoxylin and eosin (data not shown). Furthermore, hemodynamic monitoring with an indwelling Milar catheter showed that C26 treatment did not have any inhibitory effects on systolic and diastolic heart function as measured by dP/dt max and dP/dt min (Table 1). These results suggest that C26 de-

TABLE 1
Liver, kidney, and cardiac toxicity in control and C-26-treated mice ($n = 6$)

	Liver Function		Kidney Function: Urea Nitrogen	Heart Function (×1000)
	ALT	AST		
	U/l		*mM*	*dP/dt*
Control	56.6 ± 15.6	239.8 ± 31.3	11.1 ± 2.3	3.53 ± 0.40
C26	55.6 ± 17.3	233.4 ± 45.7	11.7 ± 2.2	3.54 ± 0.24

presses growth and metastasis of breast carcinoma cells in vivo and extends survival time without significant end-organ toxicity.

C26 Attenuates the Activation of Growth Factor Signaling Pathways. Western blot analysis showed that 11,12-EET (200 nM) addition up-regulated PI3 kinase and increased the phosphorylation level of the EGFR and Akt in MDA-MB-235 cells. Treatment with C26 (10 μM) had the opposite effects, which could be rescued by exogenous EET addition (Fig. 6, A–C). These data are consistent with the inhibitory effects of C26 on growth factor signaling pathways in cancer cells. C26 treatment also decreased levels of the antiapoptotic protein Bcl-2 and increased levels of the proapoptotic protein Bax (Fig. 6D), consistent with the proapoptotic effect of C26. Furthermore increased expression of the antimetastatic proteins CD82 and nm-23 were found in C26-treated cells (Fig. 6E). Numerous signal transduction pathways have been shown to regulate tumor cell biology (Anagnostopoulos et al., 2008; Kroemer and Pouyssegur, 2008). As reported previously, EETs and P450 epoxygenases induce signaling and gene expression changes that promote tumorigenic and malignant phenotypes through multiple pathways, including Bcl-2/Bax and CD82/nm-23 (Jiang et al., 2005, 2007). Thus, C26 treatment attenuated prometastatic signaling and antiapoptotic protein expression in cancer cells.

Discussion

The pathological consequences of cancer are mainly related to uncontrolled tumor growth and metastasis, both of which are a consequence of abnormal tumor cell proliferation, adhesion, invasion, and migration. Our previous studies demonstrated a role for CYP2J2-derived EETs in promoting the neoplastic phenotype of cancer cells; increased CYP2J2 expression or activity was associated with increased tumor growth and lung metastasis (Jiang et al., 2007). Given that CYP2J2 is up-regulated in human carcinoma cell lines (Jiang et al., 2005), we hypothesized that inhibition of EET production would reduce tumor growth by modifying the neoplastic phenotype of cancer cells. Herein, we have shown that a novel class of selective inhibitors of CYP2J2 has potent antitumor activity in vitro and in vivo. These terfenadone derivatives reduced human cancer cell proliferation and promoted apoptosis. They also inhibited the adhesion, migration, and invasion of cancer cells in vitro. More importantly, selective CYP2J2 inhibitors markedly attenuated the growth of a murine xenograft tumor induced by MDA-MB-435 cells in athymic BALB/c mice.

Our previous study showed that in addition to inducing tumor cell proliferation, both endogenously formed and exogenously applied EETs enhanced tumor cell motility, invasion, adhesion, prometastatic gene expression, and xenograft metastasis to lungs (Jiang et al., 2007). In the current study, we showed that selective inhibition of CYP2J2 reduces adhesion

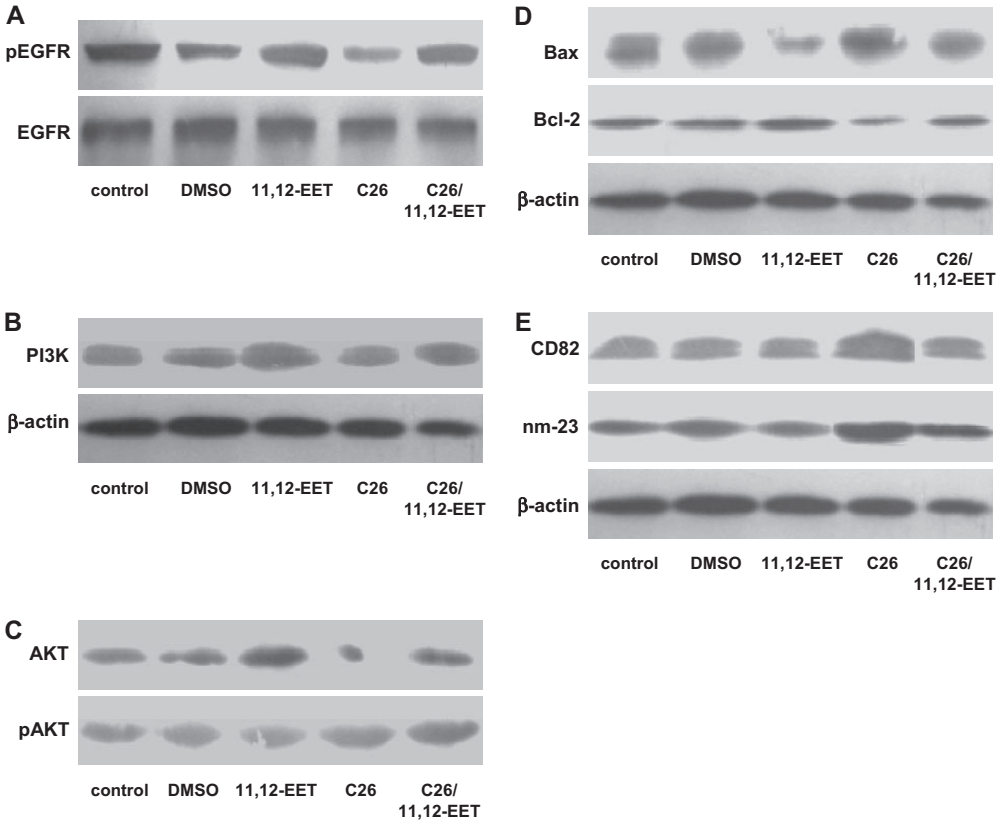

Fig. 6. Effect of C26 treatment on cell signaling pathways. MDA-MB-435 cells were treated with 200 nM EET and/or 10 μM C26 for 24 h and then analyzed for protein expression and phosphorylation. A, decreased phosphorylation of the EGFR in MDA-MB-435 cells after C26 treatment is rescued by EETs. B, decreased PI3 kinase protein expression in MDA-MB-435 cells after C26 treatment is rescued by EETs. C, decreased phosphorylation of the Akt in MDA-MB-435 cells after C26 treatment is rescued by EETs. D, effects of EET and C26 treatments on apoptosis-related proteins in MDA-MB-435 cells. E, effects of EET and C26 treatments on metastasis-related proteins in MDA-MB-435 cells.

and invasion of human tumor cells. It is important that addition of exogenous EET partially reverses these effects. Furthermore, CYP2J2 inhibition mitigated the resistance of cancer cells to apoptosis. Although not examined in this work, it is likely that the inhibition of EET production impedes the expression of the neoplastic phenotype of cells through several mechanisms. We reported previously that EETs induced endothelial nitric-oxide synthase expression and increased endothelial nitric-oxide synthase phosphorylation through activation of extracellular signal-regulated kinase and protein kinase C pathways (Wang et al., 2003). Furthermore, endogenously formed EETs protected endothelial cells from apoptosis through the extracellular signal-regulated kinase and PI3 kinase/Akt signaling pathways (Yang et al., 2007). Thus, it is likely that inhibition of these signaling pathways by the CYP2J2 inhibitors leads to the antitumor effects. Herein, we observed that C26 can slow tumor cell proliferation through inhibition of the EGFR signaling pathway, induction of tumor cell apoptosis via effects on Bax/Bcl-2 expression, and reduction of tumor cell metastasis via effects on CD82/nm23 expression. These are the same pathways previously shown to be important in P450 epoxygenase- and EET-mediated tumorigenesis and metastasis. Together, these data suggest that the antitumor activity of C26 is likely due to selective inhibition CYP2J2 enzymatic activity.

In summary, we have identified a novel class of selective inhibitors of CYP2J2 with marked antitumor properties in vitro and in vivo. The antitumor effects are associated with reduced EET biosynthesis. The observation that CYP2J2 inhibitors substantially hinder tumor growth is of potential clinical relevance. Because no signs of toxicities were observed, CYP2J2 inhibitors hold promise for use in targeted combination therapy for the control of metastatic disease. Furthermore, data demonstrating the expression of CYP2J2 in multiple cancerous tissues and the effectiveness of CYP2J2 inhibitors in various human cancer cells reveal the potential therapeutic benefit of this class of compounds in malignant diseases.

Acknowledgments

We thank Drs. Jin Kui Du and Ruo Fei Guan for efforts in CYP2J2 inhibitor synthesis.

References

Anagnostopoulos K, Tentes I, and Kortsaris AH (2008) Cell signaling in cancer. *J BUON* **13:**17–22.

Bajo AM, Schally AV, Krupa M, Hebert F, Groot K, and Szepeshazi K (2002) Bombesin antagonists inhibit growth of MDA-MB-435 estrogen-independent breast cancers and decrease the expression of the ErbB-2/HER-2 oncoprotein and c-jun and c-fos oncogenes. *Proc Natl Acad Sci U S A* **99:**3836–3841.

Bakker RA, Schoonus SB, Smit MJ, Timmerman H, and Leurs R (2001) Histamine H_1-receptor activation of nuclear factor-B: roles for G- and Gq/11-subunits in constitutive and agonist-mediated signaling. *Mol Pharmacol* **60:**1133–1142.

Capdevila JH, Falck JR, and Harris RC (2000) Cytochrome P450 and arachidonic acid bioactivation: molecular and functional properties of the arachidonate monooxygenase. *J Lipid Res* **41:**163–181.

Ciprandi G, Passalacqua G, and Canonica GW (1999) Effects of H1 antihistamines on adhesion molecules: a possible rationale for long-term treatment. *Clin Exp Allergy* **29:**49–53.

Enayetallah AE, French RA, Thibodeau MS, and Grant DF (2004) Distribution of soluble epoxide hydrolase and of cytochrome P450 2C8, 2C9, and 2J2 in human tissues. *J Histochem Cytochem* **52:**447–454.

Fishman DA, Liu Y, Ellerbroek SM, and Stack MS (2001) Lysophosphatidic acid promotes matrix metalloproteinase (MMP) activation and MMP-dependent invasion in ovarian cancer cells. *Cancer Res* **61:**3194–3199.

Jangi SM, Díaz-Pérez JL, Ochoa-Lizarralde B, Martín-Ruiz I, Asumendi A, Pérez-Yarza G, Gardeazabal J, Díaz-Ramón JL, and Boyano MD (2006) H_1 histamine receptor antagonists induce genotoxic and caspase-2-dependent apoptosis in human melanoma cells. *Carcinogenesis* **27:**1787–1796.

Jangi SM, Ruiz-Larrea MB, Nicolau-Galmés F, Andollo N, Arroyo-Berdugo Y, Ortega-Martínez I, Díaz-Pérez JL, and Boyano MD (2008) Terfenadine-induced apoptosis in human melanoma cells is mediated through Ca^{2+} homeostasis modulation and tyrosine kinase activity, independently of H_1 histamine receptors. *Carcinogenesis* **29:**500–509.

Jiang JG, Chen CL, Card JW, Yang S, Chen JX, Fu XN, Ning YG, Xiao X, Zeldin DC, and Wang DW (2005) Cytochrome P450 2J2 promotes the neoplastic phenotype of carcinoma cells and is up-regulated in human tumors. *Cancer Res* **65:**4707–4715.

Jiang JG, Ning YG, Chen C, Ma D, Liu ZJ, Yang S, Zhou J, Xiao X, Zhang XA, Edin ML, et al. (2007) Cytochrome P450 epoxygenase promotes human cancer metastasis. *Cancer Res* **67:**6665–6674.

Karara A, Makita K, Jacobson HR, Falck JR, Guengerich FP, DuBois RN, and Capdevila JH (1993) Molecular cloning, expression, and enzymatic characterization of the rat kidney cytochrome P-450 arachidonic acid epoxygenase. *J Biol Chem* **268:**13565–13570.

Kroemer G and Pouyssegur J (2008) Tumor cell metabolism: cancer's Achilles' heel. *Cancer Cell* **13:**472–482.

Kroetz DL and Zeldin DC (2002) Cytochrome P450 pathways of arachidonic acid metabolism. *Curr Opin Lipidol* **13:**273–283.

Lafite P, Dijols S, Buisson D, Macherey AC, Zeldin DC, Dansette PM, and Mansuy D (2006) Design and synthesis of selective, high-affinity inhibitors of human cytochrome P450 2J2. *Bioorg Med Chem Lett* **16:**2777–2780.

Lafite P, Dijols S, Zeldin DC, Dansette PM, and Mansuy D (2007) Selective, competitive and mechanism-based inhibitors of human cytochrome P450 2J2. *Arch Biochem Biophys* **464:**155–168.

Leurs R, Church MK, and Taglialatela M (2002) H_1-antihistamines: inverse agonism, anti-inflammatory actions and cardiac effects. *Clin Exp Allergy* **32:**489–498.

National Research Council (1996) *Guide for the care and use of laboratory animals.* National Academy Press, Washington, DC.

Node K, Huo Y, Ruan X, Yang B, Spiecker M, Ley K, Zeldin DC, and Liao JK (1999) Anti-inflammatory properties of cytochrome P450 epoxygenase-derived eicosanoids. *Science* **285:**1276–1279.

Roman RJ (2002) P-450 metabolites of arachidonic acid in the control of cardiovascular function. *Physiol Rev* **82:**131–185.

Roy S, Bayly CI, Gareau Y, Houtzager VM, Kargman S, Keen SL, Rowland K, Seiden IM, Thornberry NA, and Nicholson DW (2001) Maintenance of caspase-3 proenzyme dormancy by an intrinsic "safety catch" regulatory tripeptide. *Proc Natl Acad Sci U S A* **98:**6132–6137.

Seubert J, Yang B, Bradbury JA, Graves J, Degraff LM, Gabel S, Gooch R, Foley J, Newman J, Mao L, et al. (2004) Enhanced postischemic functional recovery in CYP2J2 transgenic hearts involves mitochondrial ATP-sensitive K^+ channels and p42/p44 MAPK pathway. *Circ Res* **95:**506–514.

Simons FE (2004) Advances in H1-antihistamines. *N Engl J Med* **351:**2203–2217.

Triggiani M, Gentile M, Secondo A, Granata F, Oriente A, Taglialatela M, Annunziato L, and Marone G (2001) Histamine induces exocytosis and IL-6 production from human lung macrophages through interaction with H_1 receptors. *J Immunol* **166:**4083–4091.

Wang H, Lin L, Jiang J, Wang Y, Lu ZY, Bradbury JA, Lih FB, Wang DW, and Zeldin DC (2003) Up-regulation of endothelial nitric-oxide synthase by endothelium-derived hyperpolarizing factor involves mitogen activated protein kinase and protein kinase C signaling pathways. *J Pharmacol Exp Ther* **307:**753–764.

Wang Y, Wei X, Xiao X, Hui R, Card JW, Carey MA, Wang DW, and Zeldin DC (2005) Arachidonic acid epoxygenase metabolites stimulate endothelial cell growth and angiogenesis via MAP kinase and PI3 kinase/Akt signaling pathways. *J Pharmacol Exp Ther* **314:**522–532.

Wu S, Chen W, Murphy E, Gabel S, Tomer KB, Foley J, Steenbergen C, Falck JR, Moomaw CR, and Zeldin DC (1997) Molecular cloning, expression, and functional significance of a cytochrome P450 highly expressed in rat heart myocytes. *J Biol Chem* **272:**272:12551–12559.

Wu S, Moomaw CR, Tomer KB, Falck JR, and Zeldin DC (1996) Molecular cloning and expression of CYP2J2, a human cytochrome P450 arachidonic acid epoxygenase highly expressed in heart. *J Biol Chem* **271:**3460–3468.

Yang S, Lin L, Chen JX, Lee CR, Seubert JM, Wang Y, Wang H, Chao ZR, Tao DD, Gong JP, et al. (2007) Cytochrome P-450 epoxygenases protect endothelial cells from apoptosis induced by tumor necrosis factor-alpha via MAPK and PI3K/Akt signaling pathways. *Am J Physiol Heart Circ Physiol* **293:**H142–H151.

Zeldin DC (2001) Epoxygenase pathways of arachidonic acid metabolism. *J Biol Chem* **276:**36059–36062.

Zipin A, Israeli-Amit M, Meshel T, Sagi-Assif O, Yron I, Lifshitz V, Bacharach E, Smorodinsky NI, Many A, Czernilofsky PA, et al. (2004) Tumor-microenvironment interactions: the fucose-generating FX enzyme controls adhesive properties of colorectal cancer cells. *Cancer Res* **64:**6571–6578.

Address correspondence to: Dr. Dao Wen Wang, Department of Internal Medicine, Tongji Hospital, Tongji Medical College, Huazhong University of Science and Technology, 1095 Jiefang Ave., Wuhan 430030, People's Republic of China. E-mail: dwwang@tjh.tjmu.edu.cn